Master's Thesis
Pricing of American Options

Erik Andreasson

August 20, 2013

Abstract

This thesis investigates the free boundary value problem of pricing American put options written on one underlying asset. In particular, attention is given to find an accurate approximation of the critical exercise boundary. The problem is approached using radial basis functions in the shape of Gaussian densities, and basis functions in the form of European put options.

Furthermore, the domain is extended into the strike direction. Prices are computed for a range of strikes and maturities, and the critical strike prices are retrieved.

Finally, the Merton Jump Diffusion model is considered generating a partial integro differential equation. Using Gaussian densities, prices and boundaries are computed on the extended domain.

Acknowledgements

I would like to thank my supervisor Magnus Wiktorsson for his valuable suggestions and contributions to this thesis.

Contents

List of Figures

List of Tables

List of Algorithms

1 Introduction

In 1973 the Chicago Board Options Exchange (CBOE) was founded; the first ever market place for trading listed options. That same year Black and Scholes (1973) published their famous paper introducing the *Black-Scholes equation*, a partial differential equation describing the dynamics of an option's value. A closed-form solution has only been obtained for European options. This implication has led to an extensive literature on pricing American options for which no general closed-form solutions exist. This problem also has some practical implications since e.g. all listed options on individual stocks in the US are American-style (Carr and Hirsa, 2003).

In the literature Analytical approximations, Monte Carlo simulation and numerical solutions such as finite differences have all been proposed for pricing American options. More recently the use of meshless methods such as radial basis functions have proved to be more easily implemented in higher dimensions, i.e. for options written on multiple underlying assets.

Furthermore, some assumptions made in Black-Scholes have also proved to be inaccurate, of which constant volatility has received most attention. Black-Scholes predicts a constant implied volatility as a function of strike and maturity, rendering a flat implied volatility surface. Empirically, the implied volatility surface tends to generate a skew or a smile. Local and stochastic volatility models both try to address this problem (Cont and Tankov, 2009, chap. 1).

There are strong empirical support for jump diffusion models when it comes to capturing these kind of characteristics. In contrast to stochastic volatility models they can explain sudden price movements exhibited in the market (Cont and Tankov, 2009, chap. 1). Merton (1976) proposed a jump diffusion model with a Poisson process generating random discrete jump times, with jump sizes following a Normal distribution. Other jump diffusion models such as the Variance Gamma (1998) and the CGMY model (2002) has later been proposed (Carr and Hirsa, 2003). The presence of a jump term in the price process of the asset generates a partial integro differential equation, which is an extension of the Black and Scholes (1973) PDE with an additional integral term.

1.1 Problem formulation

Throughout this thesis an American put option written on one underlying asset will be considered. An investor looking to purchase such an option has to specify its maturity and its strike, i.e. over what time period it can be exercised and the amount of money to be received for the asset at delivery. The investor then wants to know the price and when it is optimal to exercise the option prior to maturity. The first questions posed in this thesis are

- How can a correct price for an option be computed using a meshless method, i.e. obtaining a price for all values of the underlying asset in the computational area? What kind of functions are suitable for representing the price function? How should the grid be configured and how should parameters be chosen to improve accuracy?
- Is such a method advantageous when finding the critical exercise boundary, i.e. the rule that determines when to exercise the option?

Furthermore, the investor might be interested in purchasing a collection of options with different strikes and maturities. To avoid pricing options separately for each specific strike-maturity-pair, it would be much more convenient specifying a range of strikes and maturities for which option prices should be computed. The following questions arise

- How can prices be computed in the strike-maturity-domain for a given spot?
- Do prices computed in this extended domain agree with previous results? How well does the theoretical relation between the exercise boundary and the critical strike prices hold up?

Finally, the model is extended to include jumps. As mentioned in the introduction, this introduces an additional integral term and an extension of the Black-Scholes PDE has to be solved.

- How do suggested methods perform in this new setting? Is it possible to price options without imposing significant difficulties on the computations?

2 Theoretical foundations

2.1 The Black-Scholes model

An option is a financial instrument that gives its holder the right, but not the obligation to execute a transaction on an *underlying asset, S,* at a given point in time for a given price. The expiry date, T, is referred to as the options *maturity* and the price to be paid for the asset at maturity is called the *strike price, K,* or simply the *strike*. An option where the holder has the right to *buy* the underlying at maturity is knowns as a *call option*. Conversely, an option where the holder has the right to *sell* the underlying at maturity is known as a *put option*. Let $\Pi(S,t)$ denote the option's value at time t, then the terminal value of a call or put option is

$$\begin{aligned} \Pi^c(S,T) &= g^{call}(S) = (S-K)^+ \\ \Pi^p(S,T) &= g^{put}(S) = (K-S)^+ \end{aligned} \tag{2.1}$$

where the plus sign indicates the positive part of the parenthesis. The holder of a call option would thus earn $S_T - K$ if $S_T > K$ and zero if $S_T \leq K$. The payoffs are also depicted in Figure 1a and 1b respectively.

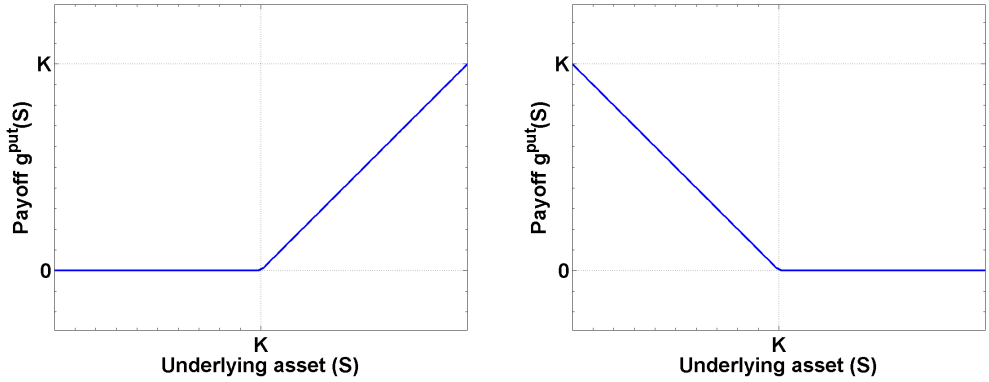

(a) Call option (b) Put option

Figure 1: Payoff functions for European call and put options. The theoretical gain from a call option is unlimited.

As can be seen from Figure 1 the theoretical gain from holding a put is limited to K while the theoretical gain from a call is unlimited. Options

like these can be used for *hedging*. Say for example that the holder of a stock is concerned that the price will plummet over the next three months. One alternative is to buy a put on that same stock, with maturity three months and some strike K. The potential loss is then limited since the holder is guaranteed K at maturity no matter how low the price of the stock has dropped. These kind of options that are only executable at maturity are called *European options*. Under the following assumptions:

- There are no arbitrage opportunities (i.e. it is not possible to make a risk free profit at zero cost).
- It is possible to borrow and lend unlimited amounts at a given risk-free rate.
- Assets are infinitely divisible.
- There are no transaction costs in buying or selling the underlying asset or the option.
- The risk free rate and the volatility are constant through time.
- The asset price, S_t, follows a geometric Brownian motion.

Black and Scholes (1973) and Merton (1973) derives a partial differential equation for European options

$$\begin{aligned} \frac{\partial \Pi}{\partial t} + (r-q)S\frac{\partial \Pi}{\partial S} + \frac{\sigma^2 S^2}{2}\frac{\partial^2 \Pi}{\partial S^2} - r\Pi &= 0 \\ \Pi(S,T) &= g(S) \end{aligned} \tag{2.2}$$

where $r \in \mathcal{R}$ is the *risk free interest rate*, $q \geq 0$ is the *continuous dividend yield* and $\sigma > 0$ is the *volatility* of the underlying asset. The authors also provide a closed form solution to equation (2.2), the famous Black-Scholes formula.[1] Under the risk neutral measure $\mathcal{Q}$, the dynamics of S_t is given by the *stochastic differential equation* (SDE)

$$dS_t = S_t(r-q)dt + S_t\sigma dW_t \tag{2.3}$$

[1] Black-Scholes formula is given in Appendix A

where $r-q$ is the *drift* and W_t is a Brownian motion. By using Itô's formula the solution to equation (2.3) is obtained

$$S_t = S_0 e^{(r-q-\frac{\sigma^2}{2})t+\sigma W_t} \tag{2.4}$$

where $S_0 > 0$ is the initial asset price. Here $\mathbb{E}^{\mathcal{Q}}[S_t] = e^{(r-q)t}S_0$ and $e^{-(r-q)t}S_t$ is thus a martingale. What equation (2.2) really says is that the discounted price of $\Pi(S,t)$ is also a martingale under the risk neutral measure $\mathcal{Q}$. Prices can therefore also be computed as expectations of their terminal value (Björk, 2009).

$$\Pi(S,t) = \mathbb{E}^{\mathcal{Q}}[e^{-r(T-t)}g(S_T)|S_t] \tag{2.5}$$

2.2 American options

An *American option* holds all the properties of the European option but with one additional feature; it can be exercised at any time t between the issuing of the option and maturity, $0 \leq t \leq T$. This slight modification complicates the option pricing problem significantly and a closed-form solution can no longer be obtained. The early exercise property of American-style options poses an interesting question; when is it optimal to exercise and when is it optimal continuing to hold the option? In fact, there exist an *optimal exercise boundary*, S^*, that separates the *exercise region*, $\mathcal{E}$, and the *continuation region*, $\mathcal{C}$. For time-invariant models, S^* depends only on time to maturity, $T-t$. It is thus the same function for *all* maturities. In the case of the American put, an *optimal stopping problem* of the form

$$\max_{0\leq t\leq T} \mathbb{E}^{\mathcal{Q}}[e^{-rt}(K-S_t)^+] \tag{2.6}$$

has to be solved. Here t is the *optimal stopping time*

$$t = \inf\{0 \leq \tau \leq T; S_\tau = S^*_{T-\tau}\} \tag{2.7}$$

i.e. the first time S_t hits S^*_{T-t}. For $S_t \leq S^*_{T-t}$ the American put should immediately be exercised. However, S^* is not known. If it was, this problem would not pose any significant new challenges. Let $V(S,t)$ be the solution to (2.6) if the following hold

- S^* is continuously differentiable, i.e. $S^* \in C^1$ and $(t, S^*_{T-t}) \in \partial\mathcal{C}$ for $t < T$

- V satisfies the PDE

$$\frac{\partial V}{\partial t} + (r-q)S\frac{\partial V}{\partial S} + \frac{\sigma^2 S^2}{2}\frac{\partial^2 V}{\partial S^2} - rV = 0,\ (S,t) \in \mathcal{C} \tag{2.8}$$

- V satisfies the final time boundary condition

$$V(S,T) = (K-S)^+,\ S \in \mathcal{R}_+ \tag{2.9}$$

- V satisfies the inequality

$$V(S,t) > (K-S)^+,\ (S,t) \in \mathcal{C} \tag{2.10}$$

- V satisfies

$$V(S,t) = (K-S)^+,\ (S,t) \in \mathcal{E} \tag{2.11}$$

- V satisfies the *smooth fit conditions*

$$\lim_{S \downarrow S^*_{T-t}} V(S,t) = K - S^*_{T-t},\ 0 \leq t < T \tag{2.12}$$

$$\lim_{S \downarrow S^*_{T-t}} \frac{\partial V}{\partial S}(S,t) = -1,\ 0 \leq t < T \tag{2.13}$$

Pricing the option is thus a *free boundary value problem*. Figure 2 depicts the *term structure* of the American put. It is clear that close to maturity $V(S,t)$ approaches the payoff function $(K-S)^+$. The optimal exercise boundary is a projection onto the St-plane of $V(S,t)$ on $\partial\mathcal{C}$. At maturity S^* is known (Björk, 2009)

$$S^*(0) = \min(1, \frac{r}{q})K \tag{2.14}$$

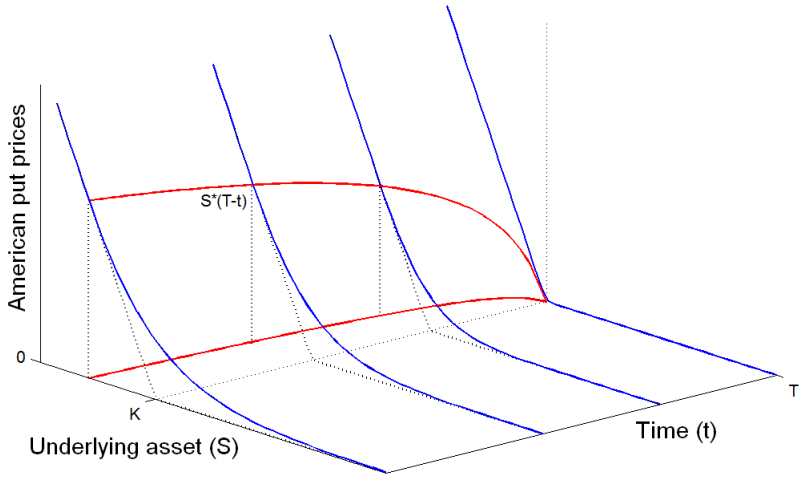

Figure 2: The term structure of the American put. The red line is the exercise boundary also projected onto the St-plane.

It can be shown that for American and European options written on the same underlying asset with the same maturity, $V(S,t) \geq \Pi(S,t)$. Since the American option holds all the properties of its corresponding European option, but with the additional early exercise premium, this is quite natural (Björk, 2009).

2.3 The perpetual American put

It is of interest to investigate the asymptotic behaviour of S^* as it gives a lower bound for where to look for the exercise boundary. Consider an option with an infinitely long maturity, i.e. $T \to \infty$. This is referred to as a perpetual option. Since the terminal date will never be reached, it is reasonable to assume that the price is independent of time, $V(S,t) = V(S)$. The free boundary value problem reduces to an *ordinary differential equation* (ODE) and the optimal exercise boundary, $S^* \equiv S^*_\infty$, is now a constant (Björk, 2009).

$$(r-q)S\frac{\partial V}{\partial S} + \frac{\sigma^2 S^2}{2}\frac{\partial^2 V}{\partial S^2} - rV = 0,\ S > S^*_\infty \tag{2.15}$$

The general solution to (2.15) has the form

$$V(S) = AS^{z_+} + BS^{z_-} \tag{2.16}$$

where

$$z_+, z_- = \frac{1}{2} - \frac{r-q}{\sigma^2} \pm \sqrt{\left(\frac{1}{2} - \frac{r-q}{\sigma^2}\right)^2 + \frac{2r}{\sigma^2}} \tag{2.17}$$

are the roots of the characteristic equation. If $q = 0$, then $z_+ = 1$ and $z_- = -\frac{2r}{\sigma^2} = -\gamma$. For a put option the condition $\lim_{S\to\infty} V(S,t) = 0$ must hold and it follows that $A = 0$, assuming a strictly positive interest rate. The boundary conditions (2.11) and (2.12) yields

$$V(S_\infty^*) = K - S_\infty^* \tag{2.18}$$

$$\lim_{S\downarrow S_\infty^*} \frac{\partial V}{S}(S) = -1 \tag{2.19}$$

and the following result is obtained

$$S_\infty^* = \frac{\gamma}{1+\gamma} K \tag{2.20}$$

for $r > 0$. It now suffices to compute the price on $[S_\infty^*, S_{\max}] \times [0, T]$ (Björk, 2009).

2.4 Upper and lower bounds

In the previous section the perpetual American put provided a limit for the critical exercise boundary. In this section the problem is further investigated by looking at American put options with finite maturity. Carr *et al.* (1992) finds an analytical expression for the American put option by decomposing the price into the corresponding European option price and an *early exercise premium* in the continuation region $\mathcal{C}$.

$$V(S,t) = v(S,t) + \epsilon_t \tag{2.21}$$

where

$$\epsilon_t = rK \int_t^T e^{-r(u-t)} \Phi\left(\frac{\ln(S_{T-u}^*/S_t) - (r - \frac{\sigma^2}{2})(u-t)}{\sigma\sqrt{u-t}}\right) du \tag{2.22}$$

and Φ denotes the standard Normal cumulative distribution function. Through the *value matching condition* (2.12), equation (2.21) implicitly solves

$$v(S^*,t) + rK \int_t^T e^{-r(u-t)} \Phi\left(\frac{\ln(S_{T-u}^*/S_t) - (r - \frac{\sigma^2}{2})(u-t)}{\sigma\sqrt{u-t}}\right) du = K - S_{T-t}^* \tag{2.23}$$

which is a non-linear integral equation with no known closed-form solution. The exercise premium, ϵ_t, is increasing in S^*_{T-t} and it is thus possible to bound the price of the American option analytically. According to the results obtained in the previous section, the exercise boundary is bounded by its asymptotic limit and the strike, $K \geq S^*_{T-t} \geq S^*_\infty$. The American put is thus bounded by

$$v(S,t) + rK \int_t^T e^{-r(u-t)} \Phi \left(\frac{\ln(K/S_t) - (r - \frac{\sigma^2}{2})(u-t)}{\sigma\sqrt{u-t}} \right) du \geq$$
$$V(S,t) \geq$$
$$v(S,t) + rK \int_t^T e^{-r(u-t)} \Phi \left(\frac{\ln(S^*_\infty/S_t) - (r - \frac{\sigma^2}{2})(u-t)}{\sigma\sqrt{u-t}} \right) du \qquad (2.24)$$

The equations given in this section has to be solved numerically and gives valuable benchmarks for comparing results obtained by methods discussed in the sequel of this report.

3 Jump models

So far trajectories of the underlying asset have been assumed to be continuous. Diffusion processes like (2.3) cannot generate discontinuous paths since the noise component, i.e. the Brownian Motion W_t, is everywhere continuous. This is clearly unrealistic since e.g. stock prices expose sudden price movements when reacting to good or bad news. In the return process this corresponds to more frequently observed outliers caused by some fat tailed underlying distribution. To reproduce a more realistic behaviour of the price process that also accounts for such movements in the price, equation (2.3) will be modified by adding a jump component. The dynamics of S become

$$\begin{aligned} dS_t =& S_{t-}(r-q)dt + S_{t-}\sigma dW_t \\ &+ \int_{-\infty}^{+\infty} (e^y - 1) S_{t-} \tilde{v}(dt, dy) \end{aligned} \qquad (3.1)$$

where

$$\tilde{v}(dt, dy) = \mu(dt, dy) - v(dt, dy) \qquad (3.2)$$

is the *compensated jump measure*. The measure $\mu(dt, dy)$ counts the number of jumps of size y at time t and $v(dt, dy)$ compensates the jump process

so that the discounted price is a martingale under the $\mathcal{Q}$-measure. Here $\int_1^\infty e^y v(dt, dy) < \infty$, $t > 0$, is a necessary no arbitrage condition. Adding a jump component to equation (3.1) will naturally also change equation (2.2) and pricing options will be significantly more complicated. Due to the presence of jumps a new (integral) term will be added to equation (2.3) and a *partial integro-differential equation* (PIDE) will have to be solved

$$\begin{aligned}&\frac{\partial V}{\partial t} + (r-q)S\frac{\partial V}{\partial S} + \frac{\sigma^2 S^2}{2}\frac{\partial^2 V}{\partial S^2} - rV \\ &+ \int_{-\infty}^{\infty}\left[V(Se^y, t) - V(S,t) - S(e^y - 1)\frac{\partial V}{\partial S}\right] v(dt, dy) = 0 \end{aligned} \tag{3.3}$$

This equation poses new challenges because of the first term under the integral, $V(Se^y, t)$, is a *nonlocal* term that depends not only on S but the whole solution of $V(\cdot, t)$ (Cont and Tankov, 2009).

3.1 Lévy-Khintchine Theorem

Consider a Lévy process, i.e. a process with independent stationary increments, of the form

$$L_t = \gamma t + \sigma W_t + Y_t \tag{3.4}$$

where $\{W_t\}_{t\geq 0}$ is a Brownian Motion and $\{Y_t\}_{t\geq 0}$ is a pure jump component. Here $\gamma \in \mathcal{R}$ is the drift and $\sigma > 0$ is the volatility. The Lévy-Khintchine Theorem characterizes the process in equation (3.4) in terms of the characteristic function of the process.

$$\mathbb{E}[e^{iuL_t}] = e^{t\psi(u)} \tag{3.5}$$

$$\psi(u) = i\gamma u - \frac{\sigma^2 u^2}{2} + \int_{-\infty}^{\infty}\left(e^{iuy} - 1 - iuy\mathbf{1}_{|y|\leq 1}\right) v(dy) \tag{3.6}$$

Here $u \in \mathcal{R}$ and the Lévy measure v satisfies $\int_{-\infty}^{\infty} \min(1, y^2) v(dy) < \infty$ and has no mass at zero.

3.2 Merton Jump Diffusion Model

Assume that the jump process $\{Y_t\}_{t\geq 0}$ follows a compound Poisson process with normally distributed jump sizes, i.e. the framework of the Merton (1976)

jump diffusion model. In this setting the compensated jump measure in (3.2) can be written

$$\mu(dt, dy) = \sum_{k=1}^{N(T)} \delta_{T_k} \delta_{y_k} \tag{3.7}$$

$$v(dt, dy) = \lambda k(y) dy dt \tag{3.8}$$

where $\{N_t\}_{t \geq 0}$ is Poisson process with intensity λ. The Lévy density $k(y)$ is in the Merton case given by the Gaussian density

$$k(y) = \frac{1}{\sqrt{2\pi}\sigma_y} e^{-\frac{1}{2\sigma_y^2}(y-\mu_y)^2} \tag{3.9}$$

An intuition for how the measure in (3.7) works is depicted in Figure 3. Here T_k are the random jump times, and the corresponding jumps Y_k follows a Normal distribution with mean μ_y and volatility σ_y^2.

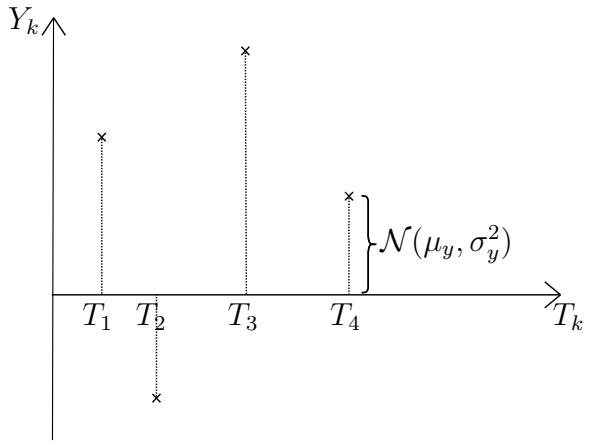

Figure 3: Jump measure in the Merton model. T_k are Poisson distributed jump times with intensity λ. Jump sizes are Normally distributed with mean μ_y and volatility σ_y^2.

Let

$$S_t = S_0 e^{L_t} \tag{3.10}$$

be the solution to equation (3.1) where L_t is the Lévy process

$$L_t = \gamma t + \sigma W_t + \sum_{k=0}^{N(t)} Y_k \tag{3.11}$$

The martingale condition, $\mathbb{E}[S_t] = S_0 e^{(r-q)t}$, is satisfied by finding the drift, γ. From equation (3.6) the following equality must hold

$$\psi(-i) = \gamma + \frac{\sigma^2}{2} + \lambda \int_{-\infty}^{\infty} (e^y - 1 - y\mathbf{1}_{|y|\leq 1})k(y)dy = r - q$$
$$\gamma = r - q - \frac{\sigma^2}{2} - \lambda \int_{-\infty}^{\infty} (e^y - 1 - y\mathbf{1}_{|y|\leq 1})k(y)dy \tag{3.12}$$

Plugging this expression for γ back into equation (3.6) yields

$$\begin{aligned}\psi(u) &= i(r - q - \frac{\sigma^2}{2})u - \frac{\sigma^2 u^2}{2} + \lambda \int_{-\infty}^{\infty} \left(e^{iuy} - 1 - iuy(e^y - 1)\right) k(y)dy \\ &= i(r - q - \frac{\sigma^2}{2} + \kappa)u - \frac{\sigma^2 u^2}{2} + \lambda \int_{-\infty}^{\infty} \left(e^{iuy} - 1\right) k(y)dy \end{aligned} \tag{3.13}$$

where

$$\kappa = -\lambda \int_{-\infty}^{\infty} (e^y - 1)k(y)dy = -\lambda(e^{\mu_y + \frac{\sigma_y^2}{2}} - 1) \tag{3.14}$$

is the *jump compensator*. It is thus clear why the compensated jump measure in equation (3.2) ensures the martingale property.

4 Extension in the strike direction

In Section 2.2 the strike price was assumed to be fixed at K. However, in practice the spot price of the asset is fixed and it is of bigger interest to price options for a range of strikes. From a traders perspective this would mean holding a number of options with different strikes, that should be exercised if some boundary related to S^* is crossed. The domain is therefore extended to all $K > 0$ and as a result $S^*(T - t, K)$ is now an *exercise surface* of all maturities and strikes $K > 0$. The PDE in (2.8) also holds in this extended domain where the price now also is a function of the strike $V(S, K, t)$. For each fixed t, the exercise boundary is a linearly homogeneous function of the strike

$$S^*(T - t, cK) = cS^*(T - t, K) \tag{4.1}$$

With $c = \frac{1}{K}$ this implies

$$KS^*(T - t, 1) = S^*(T - t, K) \tag{4.2}$$

The condition $S > S^*(T-t,K) = KS^*(T-t,1)$ is for each fixed S and t equivalent to

$$K^*(T-t,S) := \frac{SK}{S^*(T-t,K)} = \frac{S}{S^*(T-t,1)} > K \tag{4.3}$$

which is the *critical strike price*. Note that K^* depends on S but not on K. At a given time t, the trader should immediately exercise options with strikes exceeding $K^*(T-t,S)$. The critical exercise boundary S^* and the critical strike prices K^* are related as (Carr and Hirsa, 2003)

$$S^*(T-t,K)K^*(T-t,S) = SK \tag{4.4}$$

Since $V(S,K,t)$ is linearly homogeneous in S and K, i.e. for some constant c, $V(cS,cK,t) = cV(S,K,t)$, Euler's theorem states that

$$V(S,K,t) = S\frac{\partial}{\partial S}V(S,K,t) + K\frac{\partial}{\partial K}V(S,K,t) \tag{4.5}$$

(Merton, 1973). Taking derivatives of (4.5) with respect to S and K, and some rearranging of terms, yields

$$S^2\frac{\partial^2}{\partial S^2}V(S,K,t) = K^2\frac{\partial^2}{\partial K^2}V(S,K,t) \tag{4.6}$$

By substituting (4.5) and (4.6) into (3.3), the following PIDE is obtained (Carr and Hirsa, 2003)

$$\begin{aligned}&\frac{\partial V}{\partial t} - (r-q)K\frac{\partial V}{\partial K} + \frac{\sigma^2K^2}{2}\frac{\partial^2 V}{\partial K^2} - qV \\ &+ \int_{-\infty}^{\infty}\left[V(S,Ke^{-y},t) - V(S,K,t) - K(e^{-y}-1)\frac{\partial V}{\partial K}\right]e^y v(dy) = 0\end{aligned} \tag{4.7}$$

for $K < K^*(T-t,S)$. Here the linear homogeneity in the price, $V(Se^y,K,t) = e^yV(S,Ke^{-y},t)$ has been used. For a fixed $S = S_0$ and $V(S_0,K,t) := V(K,t)$, the PIDE can be solved in the Kt domain. In Section 2.2, equations (2.9) - (2.13) become

- V satisfies the final time boundary condition

$$V(K,T) = (K-S_0)^+,\ K > 0 \tag{4.8}$$

- V satisfies the inequality

$$V(K,t) > (K - S_0)^+,\ K < K^*(T-t) \tag{4.9}$$

- V satisfies

$$V(K,t) = (K - S_0)^+,\ K \geq K^*(T-t) \tag{4.10}$$

- V satisfies the smooth fit condition

$$\lim_{K \uparrow K^*_{T-t}} \frac{\partial V}{\partial K}(K,t) = 1,\ 0 \leq t < T \tag{4.11}$$

Note that to solve the same free boundary value problem as in Section 2.2 in the Kt domain, i.e. without jumps, the integral part of equation (4.7) is simply omitted.

5 A radial basis function approach

Since there are no known closed form solutions for pricing American-style options, an approximative method has to be applied. Methods such as *finite differences* have long been used for solving partial differential equations. Partial derivatives are replaced with a series expansion and an approximative solution can be represented at every node of the grid. Two problems immediately arise

- The solution is not known in between grid points and S^* is thus also unknown.
- Discretizing the integral in the PIDE can be non-trivial and computationally cumbersome.

To address the first bullet a meshless method is suggested. The price function is approximated as a combination of *basis functions*, ϕ_n, and *weights*, ω_n, in the following way

$$V(S,t) \approx \sum_{n=1}^{N} \omega_n(t)\phi_n(S) \tag{5.1}$$

where N is the number of basis functions. Note that when the weights have been found, the solution is known for all S in the computational area. This

will be helpful when looking for the critical exercise boundary. As for the second bullet; is it possible to choose ϕ_n in such a way that the difficulties with the integral can be circumvented? This question will be addressed in Section 5.2.

In this section *radial basis functions* will be considered (Fornberg *et al.*, 2011). A radial basis function $\phi_n(\mathbf{x}) = \phi(\|\mathbf{x} - \mathbf{c_n}\|)$ only depends on the distance from the *center point* $\mathbf{c_n}$. The *norm* is usually the *euclidean distance*. In this report one dimensional *Gaussian densities* will be used as radial basis functions, taking the following form

$$\phi_n(x) = e^{-\frac{1}{2\sigma_n^2}(x-c_n)^2} \tag{5.2}$$

Note that the scaling in the densities above are omitted since they will be absorbed by the weights. The *shape parameter*, σ_n, affects the *flatness* of the function as can be seen in Figure 4.

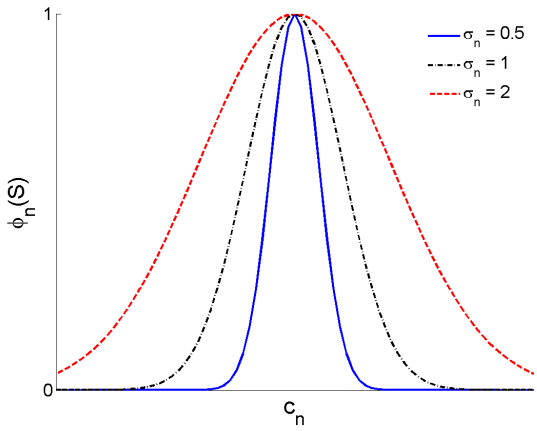

Figure 4: Gaussian densities as radial basis functions. The flatness is determined by the shape parameter σ_n.

5.1 The partial differential equation

The value of the American put is approximated as in (5.1) and the PDE in (2.8) can be written

$$-\sum_{n=1}^{N}\dot{\omega}_n(\tau)\phi_n(S)+(r-q)\sum_{n=1}^{N}\omega_n(\tau)S\frac{\partial\phi_n}{\partial S}(S) \tag{5.3}$$
$$+\frac{\sigma^2}{2}\sum_{n=1}^{N}\omega_n(\tau)S^2\frac{\partial^2\phi_n}{\partial S^2}(S)-r\sum_{n=1}^{N}\omega_n(\tau)\phi_n(S)=0,\ (S,\tau)\in\mathcal{C}$$

where the change of variables $\tau = T - t$ has been made. Here τ should be interpreted as *time to maturity*, i.e. counting backwards in time. The derivative with respect to t in (2.8)

$$\frac{\partial V}{t}(S,t)=-\frac{\partial V}{\tau}(S,\tau) \tag{5.4}$$

and the PDE is thus transformed into an *initial value problem*. In (5.3) $\dot{\omega}$ denotes the derivative with respect to τ. In order to find the weights the PDE has to be solved for different values of S. These points, S_j will be referred to as *control points*. If J different control points are chosen, (5.3) can be written

$$-\sum_{j=1}^{J}\sum_{n=1}^{N}\dot{\omega}_n(\tau)\phi_n(S_j)+(r-q)\sum_{j=1}^{J}\sum_{n=1}^{N}\omega_n(\tau)S_j\frac{\partial\phi_n}{\partial S}(S_j) \tag{5.5}$$
$$+\frac{\sigma^2}{2}\sum_{j=1}^{J}\sum_{n=1}^{N}\omega_n(\tau)S_j^2\frac{\partial^2\phi_n}{\partial S^2}(S_j)-r\sum_{j=1}^{J}\sum_{n=1}^{N}\omega_n(\tau)\phi_n(S_j)=0,\ (S_j,\tau)\in\mathcal{C}$$

or on matrix notation

$$-\mathbf{M}\dot{\boldsymbol{\omega}}(\tau)+(r-q)\mathbf{D}\boldsymbol{\omega}(\tau)+\frac{\sigma^2}{2}\mathbf{G}\boldsymbol{\omega}(\tau)-r\mathbf{M}\boldsymbol{\omega}(\tau)=0 \tag{5.6}$$

where

$$\mathbf{M} = \begin{pmatrix} \phi_1(S_1) & \phi_2(S_1) & \cdots & \phi_N(S_1) \\ \phi_1(S_2) & \phi_2(S_2) & \cdots & \phi_N(S_2) \\ \vdots & \vdots & \ddots & \vdots \\ \phi_1(S_J) & \phi_2(S_J) & \cdots & \phi_N(S_J) \end{pmatrix} \quad \mathbf{D} = \begin{pmatrix} S_1\phi_1'(S_1) & S_1\phi_2'(S_1) & \cdots & S_1\phi_N'(S_1) \\ S_2\phi_1'(S_2) & S_2\phi_2'(S_2) & \cdots & S_2\phi_N'(S_2) \\ \vdots & \vdots & \ddots & \vdots \\ S_J\phi_1'(S_J) & S_J\phi_2'(S_J) & \cdots & S_J\phi_N'(S_J) \end{pmatrix}$$

$$\boldsymbol{\omega}(\tau) = \begin{pmatrix} \omega_1(\tau) \\ \omega_2(\tau) \\ \vdots \\ \omega_N(\tau) \end{pmatrix} \qquad \mathbf{G} = \begin{pmatrix} S_1^2\phi_1''(S_1) & S_1^2\phi_2''(S_1) & \cdots & S_1^2\phi_N''(S_1) \\ S_2^2\phi_1''(S_2) & S_2^2\phi_2''(S_2) & \cdots & S_2^2\phi_N''(S_2) \\ \vdots & \vdots & \ddots & \vdots \\ S_J^2\phi_1''(S_J) & S_J^2\phi_2''(S_J) & \cdots & S_J^2\phi_N''(S_J) \end{pmatrix}$$

Equation (5.6) is discretized according to *Euler's method*

$$-\mathbf{M}\frac{\boldsymbol{\omega}(\tau_i) - \boldsymbol{\omega}(\tau_{i-\Delta_i})}{\Delta_i} + (r-q)\mathbf{D}\boldsymbol{\omega}(\tau_i) + \frac{\sigma^2}{2}\mathbf{G}\boldsymbol{\omega}(\tau_i) - r\mathbf{M}\boldsymbol{\omega}(\tau_i) = 0 \quad (5.7)$$

$$\mathbf{M}\boldsymbol{\omega}(\tau_{i-\Delta_i}) - \left[\mathbf{M} - \Delta_i\left((r-q)\mathbf{D} + \frac{\sigma^2}{2}\mathbf{G} - r\mathbf{M}\right)\right]\boldsymbol{\omega}(\tau_i) = 0 \quad (5.8)$$

The first term in equation (5.8) is identified as the known solution at time $\tau_{i-\Delta_i}$. Set

$$\mathbf{y} = \mathbf{M}\boldsymbol{\omega}(\tau_{i-\Delta_i}) \quad (5.9)$$

$$\mathbf{A}_i = \mathbf{M} - \Delta_i\left((r-q)\mathbf{D} + \frac{\sigma^2}{2}\mathbf{G} - r\mathbf{M}\right) \quad (5.10)$$

then the weights at time τ_i that minimizes the distance between the approximation and the true function values at the control points S_j, is the *least squares estimator* (LSE). Let $\boldsymbol{\omega}_0$ denote the LSE, then

$$\boldsymbol{\omega}_0(\tau_i) = \underset{\boldsymbol{\omega}_0(\tau_i)}{\arg\min} \sum_{j=1}^{J}\left(y_j - \mathbf{a}_{j,\bullet}^{(i)}\boldsymbol{\omega}_0(\tau_i)\right)^2 \quad (5.11)$$

where $\mathbf{a}_{j,\bullet}^{(i)}$ is the *jth* row of $\mathbf{A}_i$. The following function should then be minimized

$$\begin{aligned} L(\boldsymbol{\omega}_0(\tau_i)) &= \sum_{j=1}^{J}\left(y_j - \mathbf{a}_{j,\bullet}^{(i)}\boldsymbol{\omega}_0(\tau_i)\right)^2 \\ &= \mathbf{y}^\mathbf{T}\mathbf{y} - \mathbf{2}\mathbf{y}^\mathbf{T}\mathbf{A}_i\boldsymbol{\omega}_0(\tau_i) + \boldsymbol{\omega}_0(\tau_i)^T\mathbf{A}_i^T\mathbf{A}_i\boldsymbol{\omega}_0(\tau_i) \end{aligned} \quad (5.12)$$

The derivative of L should be equal to zero as a necessary condition for a minimum

$$\frac{\partial L(\boldsymbol{\omega}_0(\tau_i))}{\partial \boldsymbol{\omega}_0(\tau_i)} = -2\mathbf{A}_i^T\mathbf{y} + 2\mathbf{A}_i^T\mathbf{A}_i\boldsymbol{\omega}_0(\tau_i) = 0 \tag{5.13}$$

which gives the weights

$$\boldsymbol{\omega}(\tau_i) = (\mathbf{A}_i^T\mathbf{A}_i)^{-1}\mathbf{A}_i^T\mathbf{y} \tag{5.14}$$

So far no attention has been given to the critical exercise boundary. To get a correct representation of the price, $\omega(\tau_i)$, has to be updated once $S^*(\tau_i)$ is found. The assumption is made that the option can only be exercised at the discrete time points τ_i, i.e. the critical exercise boundary is assumed to be constant over time intervals Δ_i. According to conditions (2.10) and (2.11) the weights should be updated as

$$\begin{aligned} \mathbf{M}\boldsymbol{\omega}(\tau_i) &= \max[\mathbf{M}\boldsymbol{\omega}(\tau_i), (K_0 - \mathbf{S})^+] \\ \boldsymbol{\omega}(\tau_i) &= (\mathbf{M}^T\mathbf{M})^{-1}\mathbf{M}^T \max[\mathbf{M}\boldsymbol{\omega}(\tau_i), (K_0 - \mathbf{S})^+] \end{aligned} \tag{5.15}$$

where $\mathbf{S} = \begin{pmatrix} S_1 & \cdots & S_J \end{pmatrix}^T$ and K_0 denotes the strike. As explained in Figure 2, S^* is the projection onto the St-plane in the points where the value of the put and the payoff coincide. The area behind S^* is thus the exercise region $\mathcal{E}$. To summarize, the algorithm for pricing the American put is given by Algorithm 1.

$0 = \tau_0, \tau_1, ..., \tau_i, ..., \tau_{I-1}, \tau_I = T$;
initialize;
$\mathbf{y} = (K_0 - \mathbf{S})^+$;
$S^*_{\tau_o} = \min[1, \frac{r}{q}]K_0$;
for $i = 1 \to I$ **do**
  Compute weights;
  $\boldsymbol{\omega}(\tau_i) = (\mathbf{A}_i^T\mathbf{A}_i)^{-1}\mathbf{A}_i^T\mathbf{y}$;
  Find $S^*(\tau_i)$;
  Update weights;
  $\boldsymbol{\omega}(\tau_i) = (\mathbf{M}^T\mathbf{M})^{-1}\mathbf{M}^T \max[\mathbf{M}\boldsymbol{\omega}(\tau_i), (K_0 - \mathbf{S})^+]$;
  $\mathbf{y} = \mathbf{M}\boldsymbol{\omega}(\tau_i)$
end

Algorithm 1: Pricing of American put options in the $S\tau$ domain

The matrices $\mathbf{M}, \mathbf{D}$ and $\mathbf{G}$ for control points K_j in the $K\tau$ domain are computed analogously with

$$\mathbf{A}_i = \mathbf{M} - \Delta_i \left(-(r-q)\mathbf{D} + \frac{\sigma^2}{2}\mathbf{G} - q\mathbf{M} \right) \tag{5.16}$$

The algorithm for pricing the American put in the $K\tau$ domain is similar to Algorithm 1

$0 = \tau_0, \tau_1, ..., \tau_i, ..., \tau_{I-1}, \tau_I = T$;
initialize;
$\mathbf{y} = (\mathbf{K} - S_0)^+$;
$K^*_{\tau_0} = \frac{S_0 K_0}{S^*(\tau_0)}$;
for $i = 1 \to I$ **do**
  Compute weights;
  $\boldsymbol{\omega}(\tau_i) = (\mathbf{A}_i^T \mathbf{A}_i)^{-1} \mathbf{A}_i^T \mathbf{y}$;
  Find $K^*(\tau_i)$;
  Update weights;
  $\boldsymbol{\omega}(\tau_i) = (\mathbf{M}^T \mathbf{M})^{-1} \mathbf{M}^T \max[\mathbf{M}\boldsymbol{\omega}(\tau_i), (\mathbf{K} - S_0)^+]$;
  $\mathbf{y} = \mathbf{M}\boldsymbol{\omega}(\tau_i)$
end

Algorithm 2: Pricing of American put options in the $K\tau$ domain

Finding $S^*(\tau_i)$ and $K^*(\tau_i)$ will be discussed in Section 5.4.

5.2 The partial integro differential equation

In the Merton model, the choice of Gaussian densities as basis functions will prove to be advantageous. First, by making the change of variable $x = \ln(S)$ the terms in equation (3.3) become

$$\begin{aligned} u(x,\tau) &= V(S,\tau) \\ \frac{\partial u}{\partial x} &= S\frac{\partial V}{\partial S} \\ \frac{\partial^2 u}{\partial x^2} - \frac{\partial u}{\partial x} &= S^2 \frac{\partial^2 V}{\partial S^2} \\ u(x+y,\tau) &= V(Se^y,\tau) \end{aligned}$$

With this change of variables x and y are separated and it will be possible to solve the integral. The following PIDE is obtained

$$
\begin{aligned}
&-\frac{\partial u}{\partial \tau}+(r-q-\frac{\sigma^2}{2})\frac{\partial u}{\partial x}+\frac{\sigma^2}{2}\frac{\partial^2 u}{\partial x^2}-ru \\
&+\int_{-\infty}^{\infty}\left[u(x+y,\tau)-u(x,\tau)-(e^y-1)\frac{\partial u}{\partial x}\right]\lambda k(y)dy=0
\end{aligned}
\tag{5.17}
$$

The last term under the integral is identified as the jump compensator in (3.13). As the second term does not depend on y, and the density integrates to one, it can be moved outside the integral. The first term, however, has to be given some attention. First set

$$
u(x,\tau)=\sum_{n=1}^{N}\omega_n(\tau)\phi_n(x) \tag{5.18}
$$

then the PIDE can be written

$$
\begin{aligned}
&-\sum_{n=1}^{N}\dot{\omega}_n(\tau)\phi_n(x)+(r-q-\frac{\sigma^2}{2}+\kappa)\sum_{n=1}^{N}\omega_n(\tau)\frac{\partial \phi_n}{\partial x}(x) \\
&+\frac{\sigma^2}{2}\sum_{n=1}^{N}\omega_n(\tau)\frac{\partial^2 \phi_n}{\partial x^2}(x)-r\sum_{n=1}^{N}\omega_n(\tau)\phi_n(x) \\
&+\lambda\sum_{n=1}^{N}\omega_n(\tau)\left(\phi_n(x)\varphi_n(x)-\phi_n(x)\right)=0,\ (e^x,\tau)\in\mathcal{C}
\end{aligned}
\tag{5.19}
$$

Here it is assumed that the first term under the integral in equation (5.17) can be written as a product of ϕ_n and some other function φ_n that also depends on x and c_n. Note that y has been integrated out. The result is given in (5.20), for the details of the calculations the reader is referred to Appendix B.

$$
\varphi_n(x)=\frac{\sigma_n}{\sqrt{\sigma_n^2+\sigma_y^2}}\exp\left(-\frac{1}{2\sigma_y^2}\left(\mu_y^2-\frac{(\mu_y\sigma_n^2-\sigma_y^2(x-c_n))^2}{\sigma_n^2(\sigma_n^2+\sigma_y^2)}\right)\right) \tag{5.20}
$$

By choosing control points x_j, the matrices $\mathbf{M}$, $\mathbf{D}$ and $\mathbf{G}$ can be computed analogously to previous sections, but now with constant coefficients. Addi-

tionally, a new matrix is defined as the product of ϕ_n and φ_n

$$\mathbf{H} = \begin{pmatrix} \phi_1(x_1)\varphi_1(x_1) & \phi_2(x_1)\varphi_2(x_1) & \cdots & \phi_N(x_1)\varphi_N(x_1) \\ \phi_1(x_2)\varphi_1(x_2) & \phi_2(x_2)\varphi_2(x_2) & \cdots & \phi_N(x_2)\varphi_N(x_2) \\ \vdots & \vdots & \ddots & \vdots \\ \phi_1(x_J)\varphi_1(x_J) & \phi_2(x_J)\varphi_2(x_J) & \cdots & \phi_N(x_J)\varphi_N(x_J) \end{pmatrix}$$

The algorithm for pricing the put option in the Merton model is similar to Algorithm 1, with

$$\mathbf{A}_i = \mathbf{M} - \Delta_i \left((r - q - \frac{\sigma^2}{2} + \kappa)\mathbf{D} + \frac{\sigma^2}{2}\mathbf{G} - r\mathbf{M} + \lambda(\mathbf{H} - \mathbf{M}) \right) \tag{5.21}$$

In the Merton framework the asymptotics of the exercise boundary, S^*_∞, is not known. In contrast to Section 2.2 the price therefore has to be computed for a sufficiently low value on the underlying asset.

The PIDE in the $K\tau$ domain, after making the change of variable $x = \ln(K)$, is similar to equation (5.17)

$$\begin{aligned} &- \frac{\partial u}{\partial \tau} - (r - q + \frac{\sigma^2}{2})\frac{\partial u}{\partial x} + \frac{\sigma^2}{2}\frac{\partial^2 u}{\partial x^2} - qu \\ &+ \int_{-\infty}^{\infty} \left[u(x - y, \tau) - u(x, \tau) - (e^{-y} - 1)\frac{\partial u}{\partial x} \right] e^y \lambda k(y) dy = 0 \end{aligned} \tag{5.22}$$

As previously, the last term is identified as the jump compensator κ, but with a minus sign. The second term can once again be moved outside the integral, with $\int_{-\infty}^{\infty} e^y \lambda k(y) dy = e^{\mu_y + \frac{\sigma_y^2}{2}}$. The first term can still be written as a product between ϕ_n and a new function ψ_n given by

$$\psi_n(x) = \frac{\sigma_n}{\sqrt{\sigma_n^2 + \sigma_y^2}} \exp\left(-\frac{1}{2\sigma_y^2} \left(\mu_y^2 - \frac{((\mu_y + \sigma_y^2)\sigma_n^2 + \sigma_y^2(x - c_n))^2}{\sigma_n^2(\sigma_n^2 + \sigma_y^2)} \right) \right) \tag{5.23}$$

The calculations are similar to the once in the $S\tau$ domain given in Appendix B. The matrices $\mathbf{M}$, $\mathbf{D}$, $\mathbf{G}$ and $\mathbf{H}$ are calculated analogously and pricing the put option in the $K\tau$ domain is the same as in Algorithm 2 with

$$\mathbf{A}_i = \mathbf{M} - \Delta_i \left(-(r - q + \frac{\sigma^2}{2} + \kappa)\mathbf{D} + \frac{\sigma^2}{2}\mathbf{G} - q\mathbf{M} + \lambda(\mathbf{H} - e^{\mu_y + \frac{\sigma_y^2}{2}}\mathbf{M}) \right) \tag{5.24}$$

As the asymptotics of S^*_∞ is not known, neither is K^*_∞, which means that prices has to be calculated for a sufficiently high value on the strike in the $K\tau$-domain.

5.3 Grid configuration

When choosing a grid there are a number of parameters that can be adjusted to improve performance and accuracy.

- Placement of central and control points can be chosen freely
- Shape parameters can be adjusted to improve accuracy
- The number of central and control points, and the ratio between these will also affect the performance

In addition, discrete time steps can be taken equidistant or non-equidistant, and the size of the time steps will of course affect the accuracy in the Euler discretization. In the following section these kind of decisions will be discussed.

Due to the shape of the payoff function, see Figure 1, with a sharp edge at $S = K_0$, the derivative of S^* approaches $-\infty$ as $t \to T$. Capturing S^* close to maturity is therefore very difficult and a good representation of the price around K_0 is needed. This can be achieved by placing central points more dense around this critical point. Below the exercise boundary the solution is just a straight line, and for high values of S the price is zero, or close to zero. Representing the price function in these regions should therefore be relatively less challenging, and placement of central points can be more sparse. Since the number of central points, N, can be reduced by taking advantage of these kind of characteristics, as compared to an equidistant grid, the computational speed can also be improved. An example of how central points are distributed along the S-axis is illustrated in Figure 5.

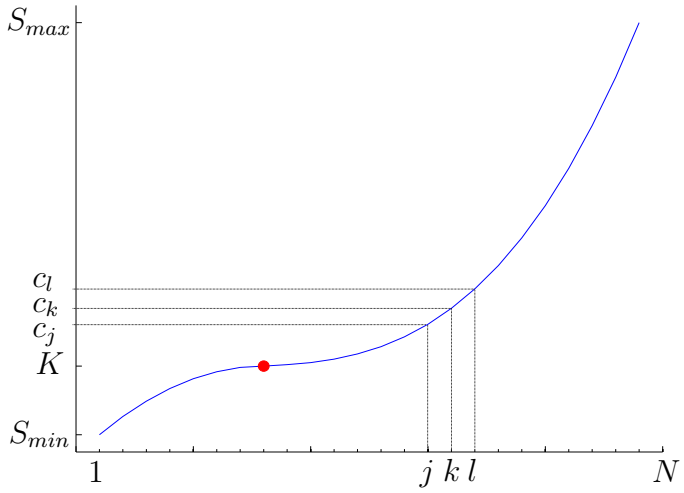

Figure 5: Distribution of central points along the S-axis. The red dot indicates the strike level.

As previously mentioned, the shape parameter, σ_n, affects the flatness of the Gaussian basis function. Empirically, the approximation improves the flatter the functions are, i.e. for high values of the shape parameter. This is quite intuitive since there will otherwise be oscillations in between central points. But there is also an upper limit for how flat the functions can be chosen to avoid rank deficiencies when computing inverses of matrices. If distances between central points are chosen non-equidistant, the flatness of each basis function should be chosen individually. In this thesis σ_n is assumed to be proportional to the distance to its nearest neighbour. For the kth basis function in Figure 5, σ_k is chosen as

$$\sigma_k \propto \min(c_k - c_j, c_l - c_k) \tag{5.25}$$

Weights are computed to minimize the distance between the approximation and the true price function in the control points. As with central points, accuracy can be improved by placing control points more dense around $S = K_0$, giving more effort in minimizing the error in this region. This in turn enables a better approximation of the critical exercise boundary close to maturity. For lower and higher values of S, control points are once again placed more sparse as it is easier to get a good representation of the price function in

these regions. For numerical reasons the number of control points should be chosen so that $J \gg N$.

When taking non-equidistant time steps, each time interval Δ_i, should increase for longer maturities to get a better approximation of the exercise boundary. Discrete time nodes t_i are generated using

$$t_i = T - \frac{n_i^k}{T^{k-1}} \tag{5.26}$$

where $k = 1, 2, 3, ...$ and $T = n_0, n_1, ..., n_{I-1}, n_I = 0$ is an equidistant grid.

5.4 Finding the exercise boundary

Pricing the option and finding the exercise boundary is done simultaneously. In the iterative pricing process, one have to keep track of the exercise boundary to get a correct approximation of the price. Over each discrete time interval it is assumed that the option will not be exercised. Once the weights have been computed, they are updated to satisfy condition (2.10) and (2.11). It is at this stage one have to keep track of the exercise boundary. Taking

$$\max[\mathbf{M}\boldsymbol{\omega}(\tau_i), (K - \mathbf{S})^+] \tag{5.27}$$

actually does the job. The first control point, in ascending order, for which $\mathbf{M}\boldsymbol{\omega}(\tau_i) > (K - \mathbf{S})^+$, is the *first* control point in the continuation region, $S^{\mathcal{C}}$. Consequently, the control point just below $S^{\mathcal{C}}$ is the *last* control point in the exercise region, $S^{\mathcal{E}}$. Since the exercise boundary is in between these two points, $S^{\mathcal{E}} \leq S^* < S^{\mathcal{C}}$, a rough approximation can be found by placing control points dense in the region where S^* is likely to be found.

In a numerical scheme like finite differences, there would be no representation of the price function in between nodes, i.e. in between $S^{\mathcal{C}}$ and $S^{\mathcal{E}}$. A more exact approximation of the exercise boundary would thus have had to involve some kind of interpolation method. However, when using basis functions a representation of the price is available for all values of S. This can clearly be exploited to find a more accurate approximation. A fixed point iteration will be implemented in the following way. By rewriting (2.11), for every fixed t

$$S = K - V(S, t) = G(S) \tag{5.28}$$

and by looping $S_{k+1} = G(S_k)$, for $k = 0, 1, 2, ...$ until convergence, S^* is obtained. The initial guess is taken as S^* at the previous time step. The iteration process is displayed in Algorithm 3 where ϵ is some tolerance level.

initial guess;
$S_g = S^*(\tau_{i-1})$;
$S_n = K - V(S_g, \tau_i)$;
while $|S_g - S_n| > \epsilon$ **do**
    $S_g = S_n$;
    $S_n = K - V(S_n, \tau_i)$;
end
$S^*(\tau_i) = S_n$

Algorithm 3: Fixed point iteration to find the exercise boundary

6 Other approaches

One of the biggest challenges faced with when pricing American-style options is finding the critical exercise boundary close to maturity. Although the use of Gaussian densities seems well fitted as basis functions, they might not be optimal when recreating the kink in the payoff function. In theory, basis functions can be chosen freely. Is it possible to find a function with more suitable characteristics?

6.1 European put options as basis functions

One function that holds exactly the properties mentioned above is the European put option. At maturity, for a given strike, it takes exactly the same shape as its American counterpart as their payoff functions are identical. The price function of the American put is therefore written as

$$V(S,t) = \sum_{n=1}^{N} \omega_n(t) \Pi^p(S,t;K_n) \tag{6.1}$$

where $\Pi^p(S,t;K_n)$ is a European put option with a given strike K_n. Note that the weights, as well as the basis functions, are time dependent. Plugging

this into equation (2.8) yields

$$\begin{aligned}&\dot{\omega}_n(t)\Pi^p(S,t;K_n)+\omega_n(t)\\&\times\underbrace{\left[\frac{\partial\Pi^p}{\partial t}+(r-q)S\frac{\partial\Pi^p}{\partial S}+\frac{\sigma^2S^2}{2}\frac{\partial^2\Pi^p}{\partial S^2}-r\Pi^p\right]}_{=0}=0\end{aligned}\tag{6.2}$$

so

$$\dot{\omega}_n(t)\Pi^p(S,t;K_n)=0\tag{6.3}$$

for $n=1,...,N$ which is a rather strange condition. The second line in the first equation is of course equal to zero since the European put obviously satisfies the Black-Scholes equation. According to equation (2.5), prices can be computed as expectations of their future value in the following way

$$\begin{aligned}&e^{-r\Delta_i}\mathbb{E}[V(S,t+\Delta_i)|\mathcal{F}_t]\\=&\sum_{n=1}^{N}e^{-r\Delta_i}\mathbb{E}\left[\omega_n(t+\Delta_i)\Pi^p(S,t+\Delta_i;K_n)|\mathcal{F}_t\right]\\=&\sum_{n=1}^{N}\omega_n(t+\Delta_i)\Pi^p(S,t;K_n)\\=&V(S,t)\end{aligned}\tag{6.4}$$

Here it is once again assumed that the critical exercise boundary is constant over Δ_i. Note that the weights are deterministic and can be moved outside the expectation. Comparing this to equation (6.1) and taking the necessary conditions in Section 2.2 into account, the following relation must hold

$$\omega_n(t)\Pi^p(S,t;K_n)=\max[\omega_n(t+\Delta_i)\Pi^p(S,t;K_n),K_0-S]\tag{6.5}$$

If control points S_j for $j=1,...,J$ are chosen, this can again be written on matrix form

$$\begin{aligned}\mathbf{M}(t)\boldsymbol{\omega}(t)&=\max[\mathbf{M}(t)\boldsymbol{\omega}(t+\Delta_i),(K_0-\mathbf{S})^+]\\\boldsymbol{\omega}(t)&=(\mathbf{M}^T(t)\mathbf{M}(t))^{-1}\mathbf{M}^T(t)\max[\mathbf{M}(t)\boldsymbol{\omega}(t+\Delta_i),(K_0-\mathbf{S})^+]\end{aligned}\tag{6.6}$$

where $\mathbf{M}(t)$ is again a $N\times J$-matrix computed as in previous sections with elements $\Pi^p(S_j,t;K_n)$. By setting $K_i=K_0$ for the ith basis function it is

possible to get an exact representation of $V(S,T)$ if $\omega_i(T) = 1$ and all other weights are zero. Note that no euler discretization is necessary using this approach. Computing $\mathbf{M}(t)$ does, however, require solving Normal distribution functions at every time step. The pricing algorithm is presented in Algorithm 4.

$T = t_I, t_{I-1}, ..., t_i, ..., t_1, t_0 = 0$;
initialize;
$S_T^* = \min[1, \frac{r}{q}]K$;
Compute $\mathbf{M}(t_{I-1})$;
Find $S^*(t_{I-1})$;
Compute weights;
$\boldsymbol{\omega}(t_{I-1}) = (\mathbf{M}^T(t_{I-1})\mathbf{M}(t_{I-1}))^{-1}\mathbf{M}^T(t_{I-1}) \max[\Pi^e(S, t_{I-1}; K), K - \mathbf{S}]$;
for $i = I - 2 \to 0$ **do**
    Compute $\mathbf{M}(t_i)$;
    Find $S^*(t_i)$;
    Compute weights;
    $\boldsymbol{\omega}(t_i) = (\mathbf{M}^T(t_i)\mathbf{M}(t_i))^{-1}\mathbf{M}^T(t_i) \max[\mathbf{M}(t_i)\boldsymbol{\omega}(t_{i+1}), K - \mathbf{S}]$;
end

Algorithm 4: Pricing of American put options using European puts

Since all weights, except for the weight corresponding to strike K_0, are zero at maturity, the approximation in the first loop is known as $\Pi^p(S, t_{I-1}; K)$.

The problem is solved analogously in the strike direction by computing European puts $\Pi^p(K, t; S_n)$ for N different spot prices. By choosing control points K_j for $j = 1, ..., J$ the matrix $\mathbf{M}(t)$ can be computed with elements $\Pi^p(K_j, t; S_n)$.

7 Results

Results are presented in the following way: In Section 7.1 and 7.2 American options as described in Section 2.2 are presented. First using radial basis functions and in the following section using European puts as basis functions. Section 7.3 contains results obtained in the Merton model using radial basis functions.

7.1 American options using RBFs

The time evolution of American put prices is presented in Figure 6. Prices are computed on $[S^*_\infty, 300]$ with $S^*_\infty = 57.1429$ taking equidistant time steps $\Delta_i = \Delta$. The figure has the expected shape of Figure 2, but with maturities on the time-axis instead of calendar time.

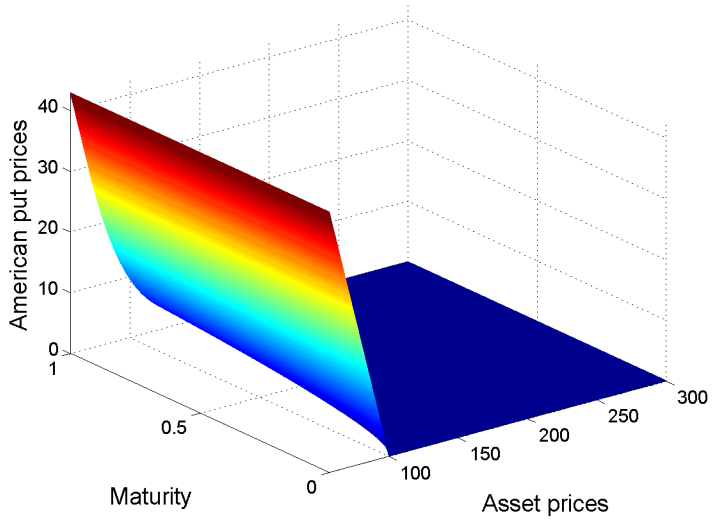

Figure 6: American put prices computed using radial basis functions with $N = 42$ central points and $J = 6 \times N$ control points taking $I = 1000$ equidistant time steps. Inputs: $r = 0.06$, $q = 0$, $\sigma = 0.3$ and $K = 100$.

As discussed in Section 2.4 upper and lower bounds can be computed solving a non-linear integral equation. The price function at time $\tau = 1$ should of course lie within these bounds to be at least somewhat accurate. As can be seen from Figure 7 the price function is located between the dashed blue lines in the region $[S^*_\infty, 160]$, this is also true for higher values of S. On the upper end of the S-axis the bounds are very narrow giving a good approximation of the price. The accuracy is thus of extra importance where the distance between bounds is greater. Shifting parameters in the model also affects the bounds. Reducing e.g. the risk free rate forces the bounds to approach each other.

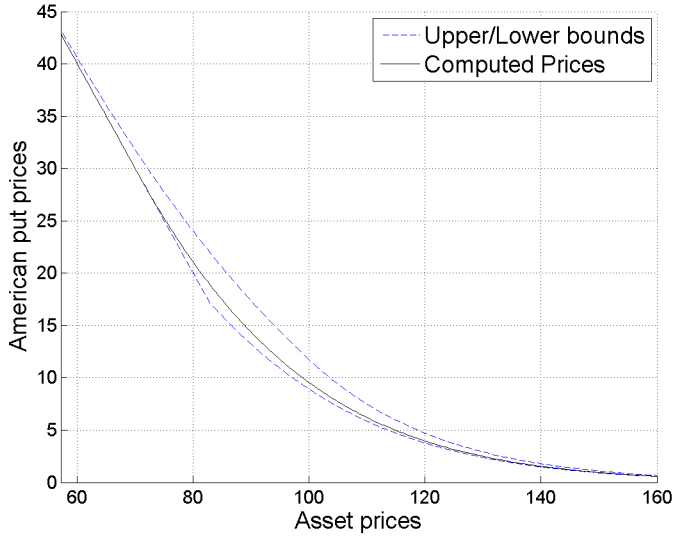

Figure 7: American put prices at time $\tau = 1$. The computed price function is located between the upper and lower bounds.

In the computations, the critical exercise boundary is assumed to be constant over discrete time intervals Δ. In reality, the option can of course be exercised at any point in time before maturity. The assumption should therefore hold more true when reducing Δ, which in turn should improve accuracy. Critical exercise boundaries for different number of time steps are depicted in Figure 8.

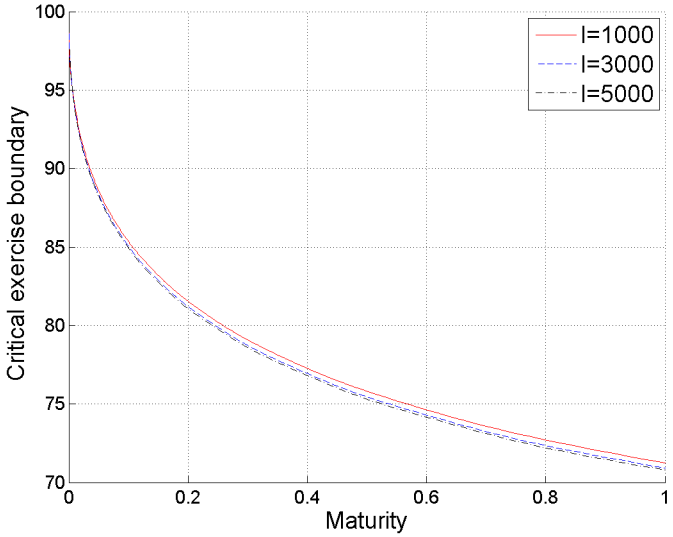

Figure 8: Critical exercise boundaries computed using radial basis function with fixed point iteration. The tolerance is set to $\epsilon = 10^{-3}$.

As the number of steps increase the exercise boundary is pushed downwards. There seems to be convergence around $I = 3000$ as this tendency is less prominent when increasing the number of steps to $I = 5000$.

American put prices computed in the strike direction are presented in Figure 9. Prices are computed on $[10, K_\infty^*]$ where $K_\infty^* = 175$. In Table 1 prices are compared to those obtained in the $S\tau$-plane. Prices agree fairly well and approach each other when moving from $I = 1000$ to $I = 3000$ steps. This underpins the conclusion that the exercise boundary converges.

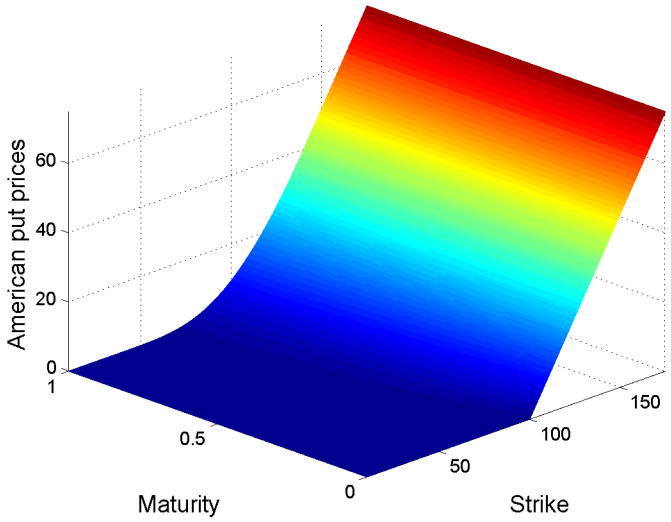

Figure 9: American put prices computed in the strike direction using radial basis functions with $N = 42$ central points and $J = 6 \times N$ control points taking $I = 1000$ equidistant time steps. Inputs: $r = 0.06$, $q = 0$, $\sigma = 0.3$ and $S_0 = 100$.

	Radial basis functions		
$I =$	1000	3000	5000
$S\tau$-plane	9.5273	9.5300	9.5305
$K\tau$-plane	9.5280	9.5305	9.5310

Table 1: American put prices in the spot and strike direction. Prices are computed for spot $S_0 = 100$ and strike $K_0 = 100$ taking I time steps. Remaining inputs are: $r = 0.06$, $q = 0$ and $\sigma = 0.3$

Critical strike prices, depicted in Figure 10a, are pushed upwards when decreasing Δ. This is consistent with the behaviour of the critical exercise boundary. To confirm the theoretical relation suggested by equation (4.4), $\frac{S^*K^*}{S_0K_0}$ is plotted in Figure 10b. This quantity should be equal to one for all maturities $\tau \in [0, 1]$. The relation holds up although one can observe some oscillations. This can be explained by small oscillation between central points in the price function. If S^* and K^* are both over- or underestimated, the error is magnified.

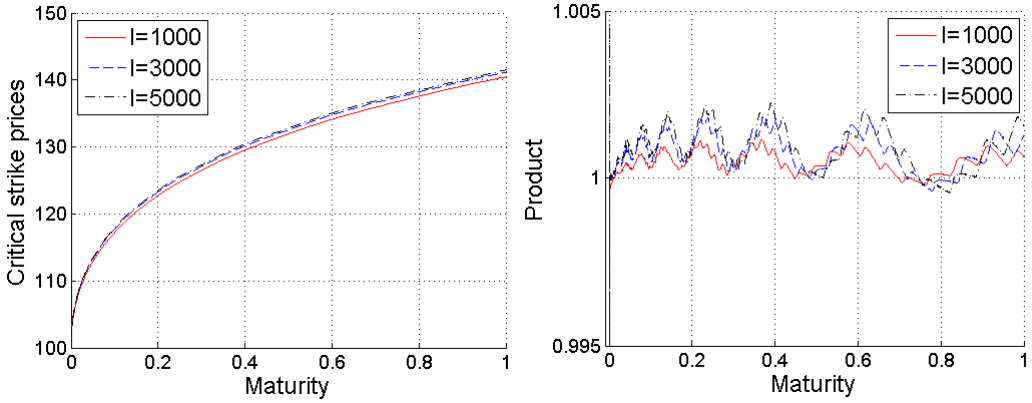

(a) Critical strike prices

(b) $\frac{S^* K^*}{S_0 K_0}$

Figure 10: Computed critical strike prices and the relation to the critical exercise boundary. Tolerance is set to $\epsilon = 10^{-3}$. The scaled product should be equal to one.

Increasing the number of time steps improves accuracy, but it also aggravates the problem of finding the exercise boundary close to maturity, see Figure 11a. For $I = 3000$ and $I = 5000$ the boundary looks unstable for short maturities and it exhibits a shape with a dint that should not be there. Although the boundary seems more stable when taking $I = 1000$ steps, the approximation is poor. Performance seems to improve in Figure 11b. Critical strike prices looks more trustworthy when increasing the number of steps.

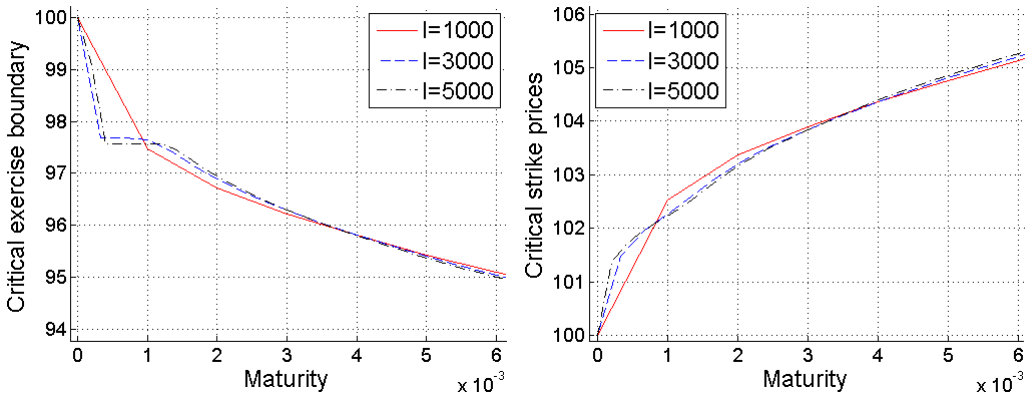

(a) Critical exercise boundary (b) Critical strike prices

Figure 11: Critical exercise boundaries and critical strikes prices for short maturities.

7.2 American options using European puts

The two different term structures of the American put are presented in Figure 12. Prices are once again computed on $[S^*_\infty, 300]$ and $[10, K^*_\infty]$ respectively with control points distributed equidistant over these regions. Non-equidistant time steps are taken according to equation (5.26) with $k = 5$.

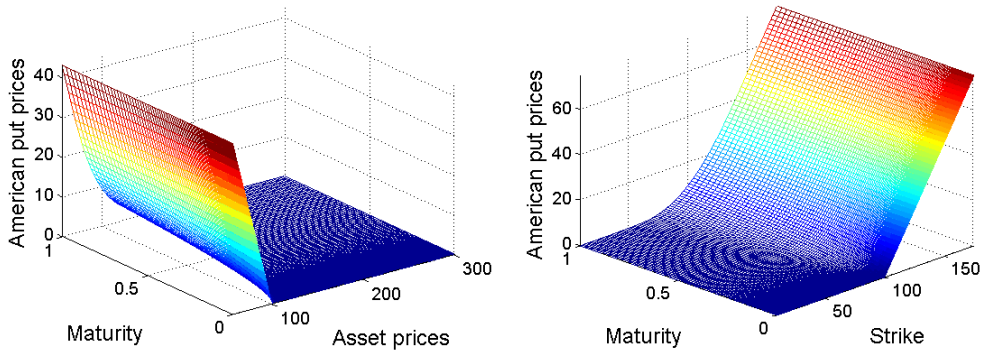

(a) Prices in the $S\tau$-plane (b) Prices in the $K\tau$-plane

Figure 12: American put prices computed using $N = 7$ European puts as basis functions, $J = 100$ control points taking $I = 200$ non-equidistant time steps. Inputs: $r = 0.06$, $q = 0$ and $\sigma = 0.3$.

Figure 13 pictures American put prices at $t = 0$. Once again prices are located between the upper and lower bounds in the region $[S^*_\infty, 160]$. For asset prices above $S = 160$, the price function crosses the upper bound (not pictured), producing incorrect prices.

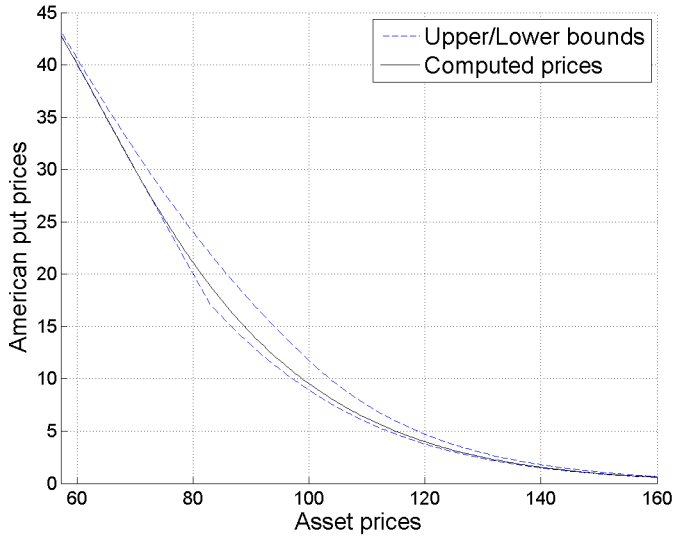

Figure 13: American put prices at $t = 0$. The price function is located in between the dashed blue lines in the pictured region.

Comparing the exercise boundary obtained in this section with the one obtained using RBFs, Figure 14a, they clearly do not coincide for longer maturities. This is not necessarily a consequence of the methods inability to produce correct prices for high asset values, as incorrect prices in this region does not affect the exercise boundary. But it does mean that prices for longer maturities cannot be trusted. Critical strike prices, Figure 14b, inherits the described problem. The theoretical relation between the exercise boundary and the strike prices, Figure 14c, holds up fairly well. The implementation of a fixed point iteration scheme to find the exercise boundary using this approach is very time consuming. For each iteration, $N \times J$ normal distribution functions have to be computed which is far from optimal.

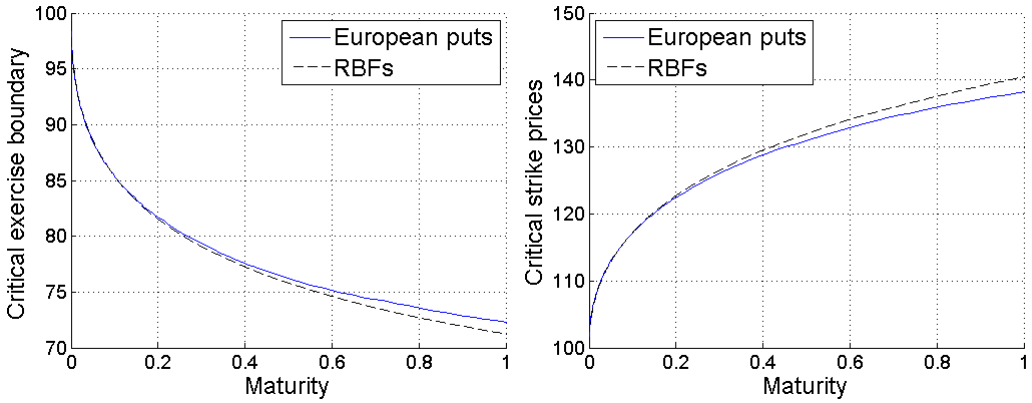

(a) Critical exercise boundary

(b) Critical strike prices

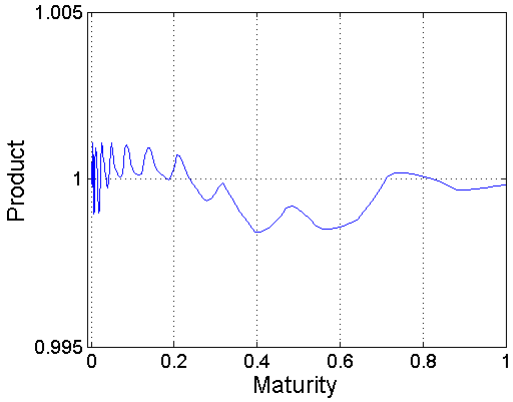

(c) $\frac{S^*K^*}{S_0K_0}$

Figure 14: Critical exercise boundary and critical strike prices computed using European puts as basis functions. The scaled product in Figure (c) should be equal to one.

Expectations were that European puts would be better at approximating the price function for short maturities. By using a non-equidistant time grid accuracy should be further improved. Figure 15a and 15b exhibits the exercise boundary and critical strike prices for short maturities. The method produces smooth curves, and seems to do a better job than Gaussian densities.

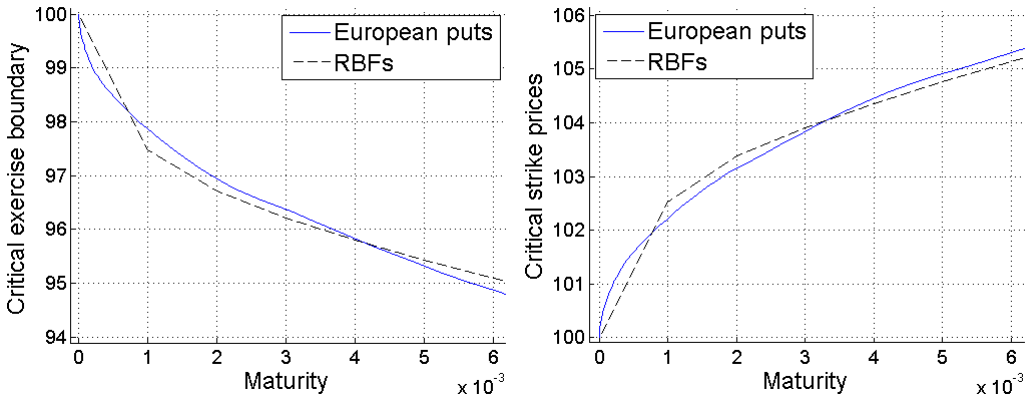

(a) Critical exercise boundary (b) Critical strike prices

Figure 15: Critical exercise boundaries and critical strike prices for short maturities.

Prices computed using European puts deviates a bit from prices computed using radial basis functions, Table 2. Regardless the accuracy obtained for at the money options using this approximation, out of the money option prices will be much more inaccurate. It should also be noted that the computational time (including the fixed point iteration) using radial basis functions taking $I = 5000$, is roughly five seconds. Despite just taking $I = 200$ steps using Europeans puts, the computational time is about four times as long.

	Radial basis functions			**European puts**
$I =$	1000	3000	5000	200
$S\tau$-plane	9.5273	9.5300	9.5305	9.5178
$K\tau$-plane	9.5280	9.5305	9.5310	9.5348

Table 2: American put prices computed using RBFs and European puts as basis functions. Prices are computed for spot $S_0 = 100$ and strike $K_0 = 100$ taking I time steps. Remaining inputs are: $r = 0.06$, $q = 0$ and $\sigma = 0.3$.

7.3 Merton Jump Diffusion Model

American put prices in the Merton model are presented in Figure 16. Prices are computed on $[10, 400]$ taking equidistant time steps. In this framework, the asymptotic behaviour of the exercise boundary is unknown. A sufficiently

low value on S therefore has to be included to make sure the boundary does not drop below the computational area.

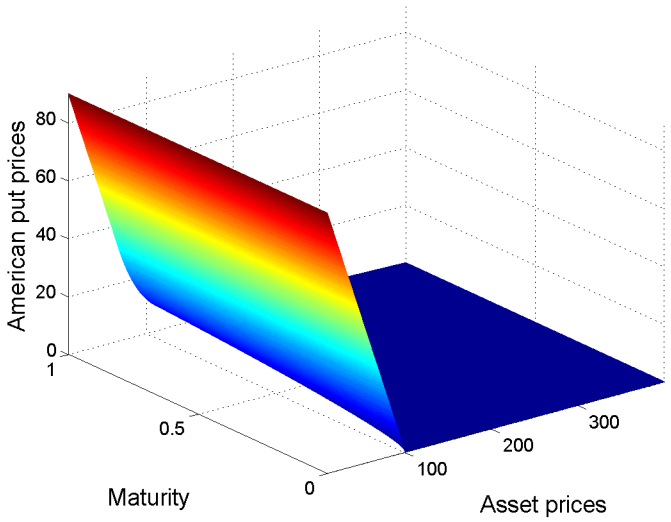

Figure 16: American put prices computed in the Merton model using radial basis functions. The method uses $N = 52$ central points and $J = 6 \times N$ control points taking $I = 1000$ equidistant time steps. Inputs: $r = 0.06$, $q = 0$, $\sigma = 0.3$, $K_0 = 100$, $\lambda = 0.1$, $\mu_y = -0.9$ and $\sigma_y = 0.45$.

The exercise boundary is depicted in Figure 17. Just like in Section 7.1, it seems to converge when increasing the number of steps. The shape of the boundary looks similar to the one in Figure 8, but it is pushed a bit further downwards ending just below $S = 70$ at $\tau = 1$. Adding jumps makes sudden positive price movements in the underlying asset possible, and the holder is therefore prepared to keep the option alive for lower values of S.

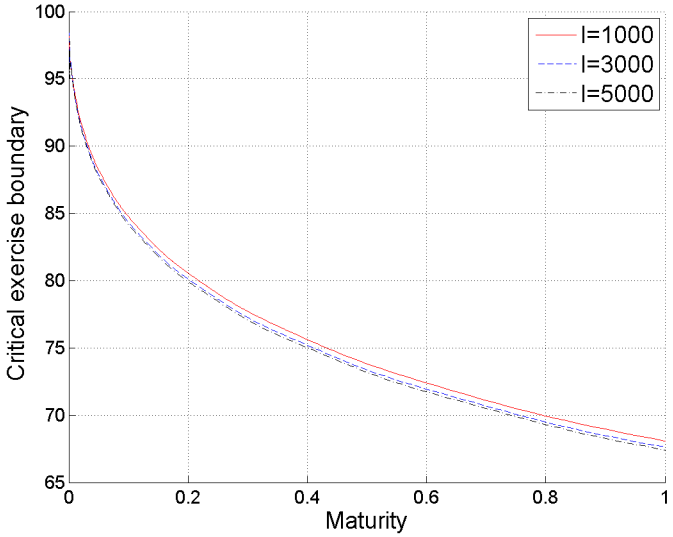

Figure 17: Critical exercise boundary in the Merton model computed taking I time steps. The boundary seems to converge when decreasing Δ.

American put prices in the strike direction are presented in Figure 18. Prices are computed on $[10, 400]$ taking equidistant time steps. As S^*_∞ is not known in the Merton model, neither is K^*_∞. For that reason a sufficiently high value on K has to be included. Comparisons between computed prices are presented in Table 3. Although prices approach each other when increasing the number of steps, they still deviate quite a lot compared to the results in Table 1.

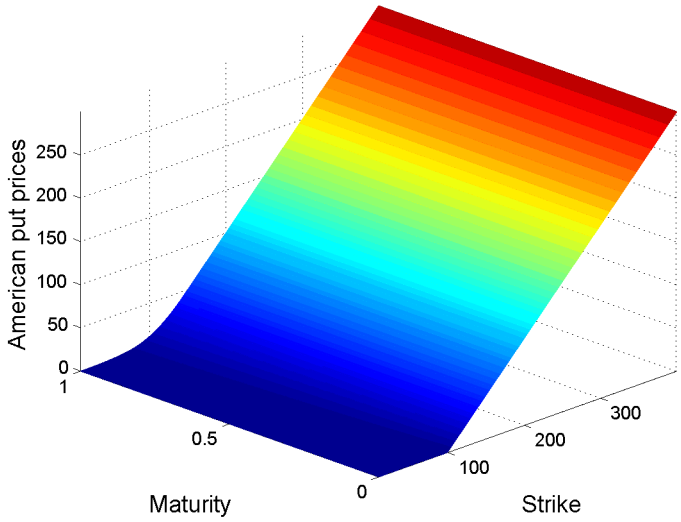

Figure 18: American put prices computed in the Merton model using radial basis functions in the strike direction. The method uses $N = 52$ central points and $J = 6 \times N$ control points taking $I = 1000$ equidistant time steps. Inputs: $r = 0.06$, $q = 0$, $\sigma = 0.3$, $S_0 = 100$, $\lambda = 0.1$, $\mu_y = -0.9$ and $\sigma_y = 0.45$.

	Radial basis functions		
$I =$	1000	3000	5000
$S\tau$-plane	11.7523	11.7556	11.7563
$K\tau$-plane	11.7067	11.7159	11.7186

Table 3: American put prices computed for spot $S_0 = 100$ and strike $K_0 = 100$ taking I time steps. Inputs: $r = 0.06$, $q = 0$, $\sigma = 0.3$, $\lambda = 0.1$, $\mu_y = -0.9$ and $\sigma_y = 0.45$.

Critical strike prices in Figure 19a clearly shifts a bit more than the corresponding exercise boundary when increasing the number of time steps. The product in Figure 19b still makes small deviations from one, but tends to increase for longer maturities. This could of course explain the price differences in Table 3 which are computed for $\tau = 1$.

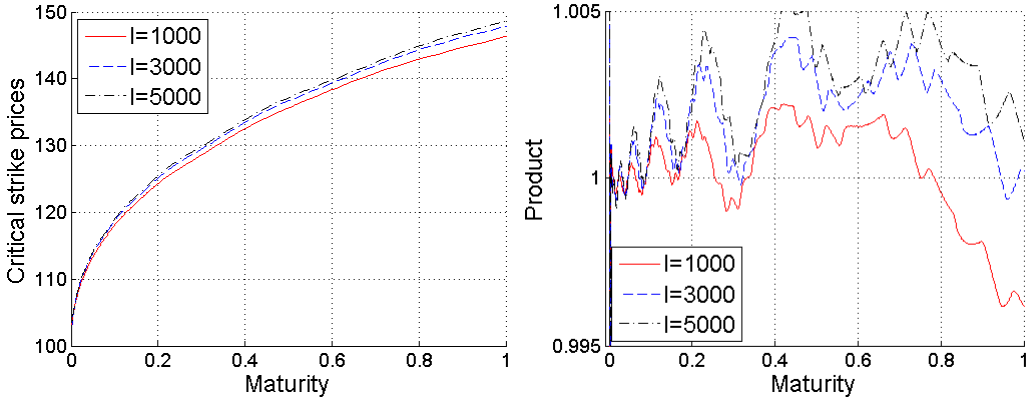

(a) Critical strike (b) $\frac{S^*K^*}{SK}$

Figure 19: Critical strike prices in the Merton model and its scaled product with the critical exercise boundary.

The Gaussian densities seems to be unable to capture the exercise boundary for short maturities in Figure 20a. The error is amplified when reducing Δ. This problem is not as prominent in Figure 20b, and the approximation seems to do a better job in the strike direction yet again.

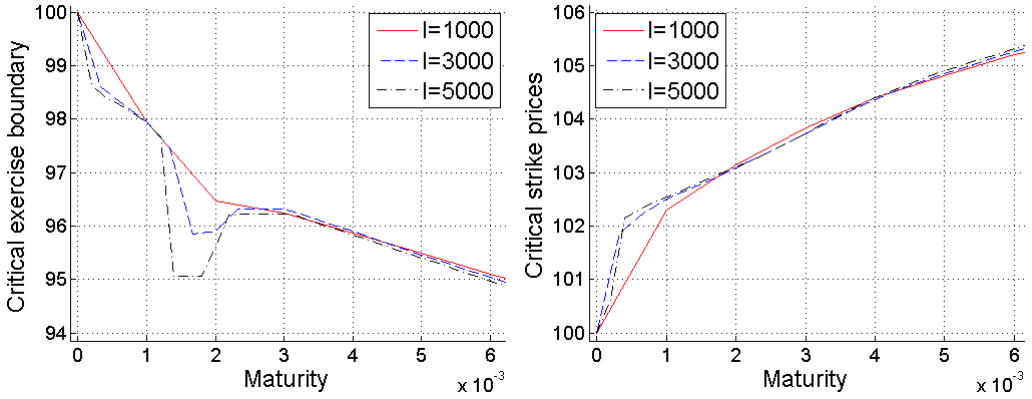

(a) Critical exercise boundary (b) Critical strike prices

Figure 20: Critical exercise boundary and critical strike prices close to maturity.

The problem occurring in Figure 20a can be explained by looking at

Figure 21 where $V - (K - S)^+$ after the first iteration is depicted. The solution in the Merton model, Figure 21b, looks very unstable exhibiting strong oscillations. It is therefore not clear to what value the fixed point iteration will converge, this of course, depends on where it starts looking for the boundary. If the starting value is too low, the error will linger until the iteration converges to a correct value in some subsequent loop.

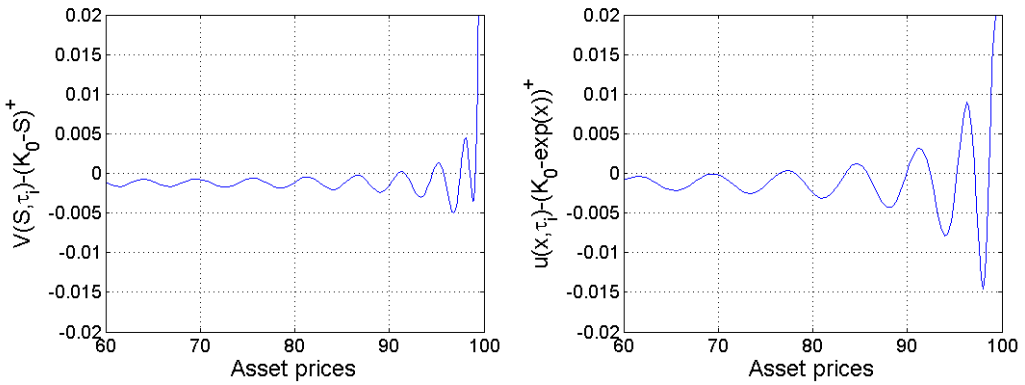

(a) Plain American put (b) Merton model

Figure 21: Price function oscillations in the first iteration taking $I = 5000$ time steps. The solution in the Merton model, Figure (b), looks more unstable.

Oscillations are present when computing prices in the strike direction, Figure 22, but they appear to be a lot less prominent. For longer maturities the oscillations fade away, an retrieving the boundary becomes a much easier task.

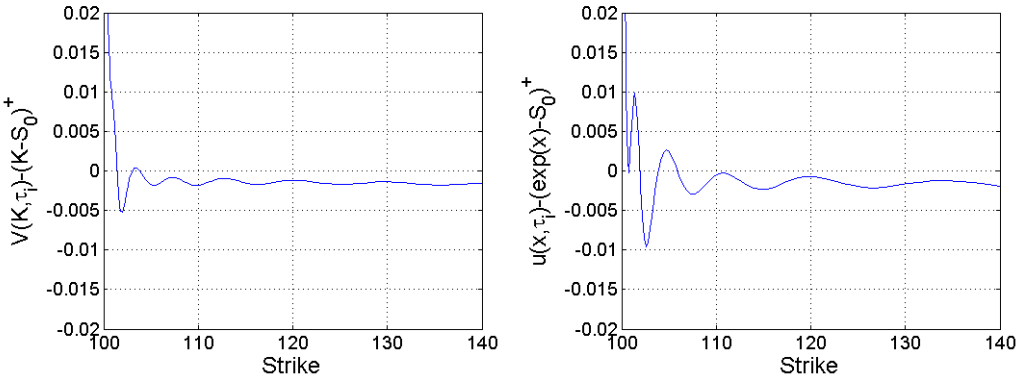

(a) Plain American put (b) Merton model

Figure 22: Price function oscillations in the strike direction. The figure pictures the first iteration taking $I = 5000$ time steps.

8 Summary

8.1 Conclusion

- Gaussian densities as radial basis functions are in many ways suitable for option pricing. The one significant drawback is the difficulty of retrieving a correct representation of the price function as $t \to T$. Consequently, the critical exercise boundary cannot be found accurately for short maturities. Although European put options as basis function are better suited for this task, it is not a good solution as they provide incorrect prices and critical exercise levels for longer maturities.

- Dense placement of central points in the region where one would expect to find the exercise boundary seems to provide good results. Empirically, the magnitude of the shape parameter should roughly be chosen as big as possible, i.e. without getting strange prices or rank deficiencies. Placement of control points is not as essential as long as there are sufficiently many. Of course, an unnecessary amount only slows down the code and for that reason they should be distributed in a smart way.

  Increasing the number of time steps forces the critical exercise boundary to converge. There is, however, a limit for how hard one can stress the algorithm for short maturities without getting erroneous results. It is, of course, in this region where the boundary is steep one would benefit the most by reducing step sizes. A more accurate approximation of the boundary, and the price, further from maturity seems to come at the price of inaccurate results close to maturity, and additional computational time.

- Empirically, if a good approximation of the exercise boundary is found, it will also provide accurate prices. However, a poor representation of the exercise boundary does not necessarily impose large deviations in the price. This relation emphasises the difficulties provided by this problem.

- Using a fixed point iteration scheme to find the exercise boundary works fairly well if a good representation of the price can be retrieved. If the boundary is flat, it takes only one or two iteration to reach convergence.

Close to maturity one could speed up performance by providing a better guess of where to start looking for the boundary.

- The choice of Gaussian densities as basis functions is advantageous in the Merton model as the integral can be solved, reducing the problem to basically the same as in the previous section. Including jumps alters the shape of the exercise boundary and pushes it downwards. The implemented method has bigger difficulties finding the boundary for short maturities in this framework. This is due to oscillations remaining in the solution over a range of short maturities, tricking the fixed point iteration to converge to incorrect values.

- Pricing options in the strike direction seems to work equally well. Results in this report even suggests that the boundary is more efficiently retrieved for short maturities. But it is perhaps more plausible that central points are better distributed along the K-axis. The theoretical relation between the critical exercise boundary and critical strike prices holds up and is not hard to find. As previously mentioned, this provides a convenient way of pricing a collection of options for a given spot price.

8.2 Further development

- Placement of central points have been chosen rather arbitrarily based on trial and error. A method of how these are distributed would both optimize the solution and make it more general. If parameters are changed, it is sometimes necessary to configure the grid, which is an ineffective and untenable solution.

  The magnitude of each shape parameter is in this report assumed to be proportional to the distance to its nearest neighbour. This is once again a rule based on empirical findings and might not be optimal. It is reasonable to assume that there is a connection between the number of basis functions and the magnitude of the shape parameters. Furthermore, it would be of interest finding a rule for the optimal number of basis functions to include for a given accuracy.

- Although the critical exercise level is retrieved at each iteration, this is not exploited when updating the weights. An updated grid could be

implemented containing the current exercise level above which the new prices should be computed. This would of course mean re-computing matrices at each iteration.

- By including an additional term when updating the weights, as in Carr and Hirsa (2003), it might be possible to force the exercise boundary to converge faster, obtaining more accurate prices with fewer time steps. A more sophisticated discretization scheme could also be implemented.

A Black-Scholes-Merton formula

The price of an European call and put option is given by Black-Scholes-Merton formula

$$V^{call}(S,t) = e^{-q\tau} S\Phi(d_1(S,t) - e^{-r\tau} K\Phi(d_2(S,t)) \tag{A.1}$$

$$V^{put}(S,t) = e^{-r\tau} K\Phi(-d_2(S,t)) - e^{-q\tau} S\Phi(-d_1(S,t)) \tag{A.2}$$

where

$$d_i(S,t) = \frac{1}{\sigma\sqrt{\tau}} \left(\ln\left(\frac{S}{K}\right) + \left(r - q + \frac{\sigma^2}{2}\right)\tau \right) \tag{A.3}$$

$$\begin{aligned} d_2(S,t) &= \frac{1}{\sigma\sqrt{\tau}} \left(\ln\left(\frac{S}{K}\right) - \left(r - q + \frac{\sigma^2}{2}\right)\tau \right) \\ &= d_1 - \sigma\sqrt{\tau} \end{aligned} \tag{A.4}$$

Here $\tau = T - t$, i.e. time to maturity, where T is the maturity of the option.

B Merton integral

$$\int_{-\infty}^{\infty} \phi_n(x+y)k(y)dy$$
$$= \int_{-\infty}^{\infty} e^{-\frac{1}{2\sigma_n^2}(x-c_n+y)^2} \frac{1}{\sqrt{2\pi}\sigma_y} e^{-\frac{1}{2\sigma_y^2}(y-\mu_y)^2} dy$$

separate y

$$= \exp\left(-\frac{1}{2\sigma_n^2\sigma_y^2}(\sigma_y^2(x-c_n)^2 + \sigma_n^2\mu_y^2)\right) \frac{1}{\sqrt{2\pi}\sigma_y}$$
$$\times \int_{-\infty}^{\infty} \exp\left(-\frac{1}{2\sigma_n^2\sigma_y^2}(y^2(\sigma_y^2+\sigma_n^2) + 2y(\sigma_y^2(x-c_n) - \sigma_n^2\mu_y)\right) dy$$

set $\delta_n = \sqrt{\frac{\sigma_n^2\sigma_y^2}{\sigma_n^2+\sigma_y^2}}$ and $\gamma_n(x) = \frac{\sigma_n^2\mu_y - \sigma_y^2(x-c_n)}{\sigma_n^2+\sigma_y^2}$

$$= \phi_n(x) \exp\left(-\frac{\mu_y^2}{2\sigma_y^2}\right) \frac{\delta_n}{\sigma_y}$$
$$\times \int_{-\infty}^{\infty} \frac{1}{\sqrt{2\pi}\delta_n} \exp\left(-\frac{1}{2\delta_n^2}(y-\gamma_n(x))\right) dy$$

completing the square

$$= \phi_n(x) \exp\left(-\frac{\mu_y^2}{2\sigma_y^2} + \frac{\gamma_n^2(x)}{2\delta_n^2})\right) \frac{\delta_n}{\sigma_y}$$
$$\times \underbrace{\int_{-\infty}^{\infty} \frac{1}{\sqrt{2\pi}\delta_n} \exp\left(-\frac{1}{2\delta_n^2}(y-\gamma_n(x))^2\right) dy}_{=1}$$
$$= \phi_n(x) \frac{\sigma_n}{\sqrt{\sigma_n^2+\sigma_y^2}} \exp\left(-\frac{1}{2\sigma_y^2}(\mu_y^2 - \frac{(\sigma_n^2\mu_y - \sigma_y^2(x-c_n))^2}{\sigma_n^2(\sigma_n^2+\sigma_y^2)}\right)$$
$$:= \phi_n(x)\varphi_n(x)$$

References

Chicago Board Options Exchange. *CBOE History*, [Online]. `http://www.cboe.com/AboutCBOE/History.aspx`. Accessed 24 July 2013.

Björk, T. 2009. *Arbitrage Theory in Continous Time*. Oxford University Press, third ed.

Black, F. and Scholes, M. 1973. The pricing of options and corporate liabilities. *The Journal of Political Economy* , Vol. 81, pp. 637–654.

Carr, P. and Hirsa, A. 2003. Why be backward? forward equations for for american options. *Risk* pp. 103–107.

Carr, P., Jarrow, R. and Myneni, R. 1992. Alternative charachterizations of american put options. *Mathematical Finance* , Vol. 2, pp. 87–106.

Cont, R. and Tankov, P. 2009. *Financial Modelling with Jump Processes*. Chapman & HALL/CRC, second ed.

Fornberg, B., Larsson, E. and Flyer, N. 2011. Stable computations with gaussian radial basis functions. *Siam journal of scientific computing* , Vol. 33(2), pp. 869–892.

Merton, R. C. 1973. Theory of rational option pricing. *The Bell Journal of Economics and Management Science* , Vol. 4, pp. 141–183.

Merton, R. C. 1976. Option pricing when underlying stock returns are discontinuous. *Journal of Financial Economics* , Vol. 3, pp. 125–144.